Inorg. Chem. **2005**, *44*, 282–292

Two Distinct Ln(III)–Cu(I) Cyanide Extended Arrays: Structures and Synthetic Methodology for Inclusion and Layer Complexes

Shengming Liu, Christine E. Plecnik, Edward A. Meyers, and Sheldon G. Shore*

Department of Chemistry, The Ohio State University, Columbus, Ohio 43210

Received September 22, 2004

Encapsulation complexes formulated as $\{[La(DMF)_9]_2[Cu_{12}(CN)_{18}]\cdot 2DMF\}_\infty$, **1**, and $\{[Ln(DMF)_8][Cu_6(CN)_9]\cdot 2DMF\}_\infty$ (Ln = Eu, **2**; Gd, **3**; Er, **4**) were obtained from the one step reaction of $LnCl_3$ (Ln = La, Eu, Gd, Er) with CuCN and KCN in DMF. They consist of a three-dimensional Cu–CN anionic array with pockets occupied by the cation, $[Ln(DMF)_x]^{3+}$ ($x = 8, 9$). These complexes are believed to be the first examples of encapsulated Ln^{3+} cations, and the zeolite-like anionic network is unique. A two step procedure that employs the same components generates the layer structure $\{Ln(DMF)_4Cu_2(CN)_5\}_\infty$ (Ln = La, **5**; Gd, **6**; Er, **7**) in which the five-membered ring repeating unit has Cu–CN–Ln and Cu–CN–Cu linkages which are also without precedent. Encapsulation complexes can also be prepared from CuCl, reacting with $LnCl_3$ and KCN. The crystal structure of $\{K(DMF)_2Cu(CN)_2\}_\infty$ (**8**) provides insight into the proposed reaction pathways for forming these two different structural types.

Introduction

It is becoming increasingly apparent that lanthanide–transition-metal (Ln–M) complexes offer a wide variety of structural possibilities, some of which might be useful in the realization of applications in materials science[1,2] and catalysis.[3] Therefore, it is advantageous to expand structural and chemical knowledge through the preparation and evaluation of new types of Ln–M systems. This goal prompted us to extend our Ln–M studies from group 10 cyanometalates ($[M(CN)_4]^{2-}$; M = Ni, Pd, Pt)[4] to group 11 Cu(I) cyanides.

In previous investigations, Ln–M(group 10) cyanides were synthesized by two alternate metathesis reactions (eqs 1, 2; Ln/M ratio is 2:3). Although both reactions generate identical products, eq 2 is the more attractive procedure because the transition metal cyanometalate reagents in eq 1 are expensive and it is difficult to remove water of crystallization from $K_2[M(CN)_4]$.

$$2LnCl_3 + 3K_2[M(CN)_4] \xrightarrow[-6KCl]{DMF} \{(DMF)_xLn_2[M(CN)_4]_3\}_\infty \quad \begin{matrix} M = Ni, Pd, Pt \\ x = 10, 13 \\ \text{type A, B, C structures} \end{matrix} \quad (1)$$

$$2LnCl_3 + 3MCl_2 + 12KCN \xrightarrow[-12KCl]{DMF} \{(DMF)_xLn_2[M(CN)_4]_3\}_\infty \quad \begin{matrix} M = Ni, Pd, Pt \\ x = 10, 12 \\ \text{type A, B, C structures} \end{matrix} \quad (2)$$

Depending upon the crystallization conditions and the lanthanide employed, one of three structural classes, types

* To whom correspondence should be addressed. E-mail: shore@chemistry.ohio-state.edu.

(1) For electroceramic and chemical sensor studies, please see: (a) Shuk, P.; Vecher, A.; Kharton, V.; Tichonova, L.; Wiemhöfer, H. D.; Guth, U.; Göpel, W. *Sens. Actuators, B* **1993**, *16*, 401–405. (b) Sadaoka, Y.; Traversa, E.; Sakamoto, M. *J. Mater. Chem.* **1996**, *6* (8), 1355–1360. (c) Traversa, E.; Matsushima, S.; Okada, G.; Sadaoka, Y.; Sakai, Y.; Watanabe, K. *Sens. Actuators, B* **1995**, *25*, 661–664. (d) Matuura, Y.; Matsushima, S.; Sakamoto, M.; Sadaoka, Y. *J. Mater. Chem.* **1993**, *3* (7), 767–769.

(2) For fluorescent and rear earth orthoferrite material studies, please see: (a) Sakamoto, M.; Matsuki, K.; Ohsumi, R.; Nakayama, Y.; Matsumoto, A.; Okawa, H. *Bull. Chem. Soc. Jpn.* **1992**, *65*, 2278–2279. (b) Gallagher, P. K. *Mater. Res. Bull.* **1968**, *3*, 225–232. (c) Sadaoka, Y.; Aono, H.; Traversa, E.; Sakamoto, M. *J. Alloys Compd.* **1998**, *278*, 135–141 and references therein.

(3) (a) Imamura, H.; Miura, Y.; Fujita, K.; Sakata, Y.; Tsuchiya, S. *J. Mol. Catal. A* **1999**, *140*, 81–90. (b) Imamura, H.; Igawa, K.; Sakata, Y.; Tsuchiya, S. *Bull. Chem. Soc. Jpn.* **1996**, *69*, 325–331. (c) Imamura, H.; Igawa, K.; Kasuga, Y.; Sakata, Y.; Tsuchiya, S. *J. Chem. Soc., Faraday Trans.* **1994**, *90*, 2119–2124. (d) Rath, A.; Liu, J.; Shore, S. G.; Aceves, E.; Mitome, J.; Ozkan, U. S. *J. Mol. Catal. A: Chem.* **2001**, *165*, 103–111. (e) Shore, S. G.; Ding, E.; Park, C.; Keane, M. A. *Catal. Commun.* **2002**, *3*, 77–84. (f) Shore, S. G.; Ding, E.; Park, C.; Keane, M. A. *J. Mol. Catal. A: Chem.* **2004**, *212*, 291–300. (g) Jujjuri, S.; Ding, E.; Shore, S. G.; Kean, M. A. *Appl. Organomet. Chem.* **2003**, *17*, 493–498.

(4) (a) Plecnik, C.; Liu, S.; Shore, S. G. *Acc. Chem. Res.* **2003**, *36*, 499–508. (b) Liu, J.; Knoeppel, D. W.; Liu, S.; Meyers, E. A.; Shore, S. G. *Inorg. Chem.* **2001**, *40*, 2842–2850. (c) Du, B.; Meyers, E. A.; Shore, S. G. *Inorg. Chem.* **2001**, *40*, 4353–4360. (d) Du, B.; Meyers, E. A.; Shore, S. G. *Inorg. Chem.* **2000**, *39*, 4639–4645. (e) Knoeppel, D. W.; Liu, J.; Meyers, E. A.; Shore, S. G. *Inorg. Chem.* **1998**, *37*, 4828–4837. (f) Knoeppel, D. W.; Meyers, E. A.; Shore, S. G. *Inorg. Chem.* **1996**, *35*, 1747–1748.

10.1021/ic040113+ CCC: $30.25
Published on Web 12/29/2004

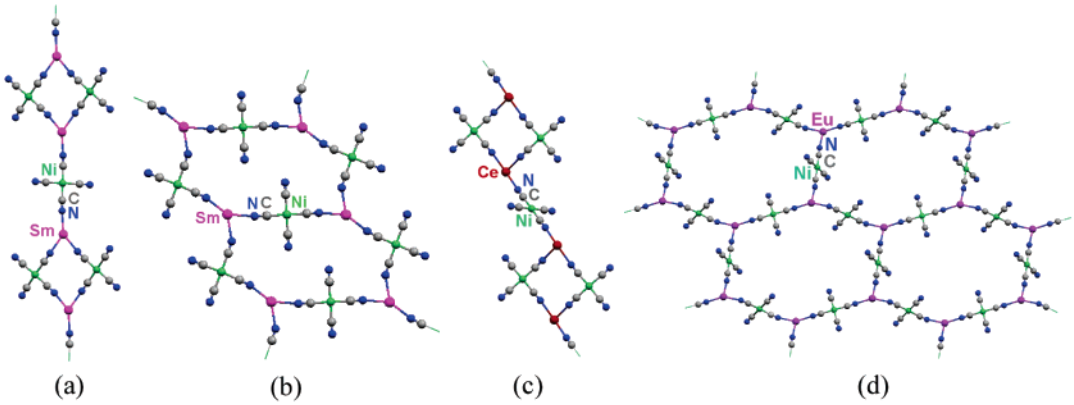

Figure 1. (a) Type A 1-D single-strand chain of $\{(DMF)_{10}Ln_2[M(CN)_4]_3\}_\infty$ (Ln = Sm, M = Ni). (b) Type B 1-D double-strand chain of $\{(DMF)_{10}Ln_2[M(CN)_4]_3\}_\infty$ (Ln = Sm, M = Ni). (c) Type C 1-D zigzag chain of $\{(DMF)_{10}Ln_2[M(CN)_4]_3\}_\infty$ (Ln = C3, M = Ni). (d) 2-D puckered sheet, $\{(DMF)_{10}Ln_2[M(CN)_4]_3\}_\infty$, in $\{(DMF)_{10}Ln_2[M(CN)_4]_3{\cdot}K_2(DMF)_4[Ni(CN)_4]\}_\infty$ (Ln = Eu, M = Ni).

Table 1. Crystallographic Data for $\{[La(DMF)_9]_2[Cu_{12}(CN)_{18}]{\cdot}2DMF\}_\infty$, **1**, $\{[Ln(DMF)_8][Cu_6(CN)_9]{\cdot}2DMF\}_\infty$[a] (Ln = Eu, **2**; Er, **4**)

	1	**2**	**4**
empirical formula	$C_{78}H_{140}Cu_{12}La_2N_{38}O_{20}$	$C_{39}H_{70}Cu_6EuN_{19}O_{10}$	$C_{39}H_{70}Cu_6ErN_{19}O_{10}$
fw	2970.58	1498.34	1513.64
cryst syst	monoclinic	monoclinic	monoclinic
space group	$P2_1/c$	$P2_1/c$	$P2_1/c$
a, Å	27.112(1)	15.133(1)	15.081(1)
b, Å	17.070(1)	15.729(1)	15.682(1)
c, Å	27.561(1)	27.288(1)	27.302(1)
β, deg	101.52(1)	101.40(1)	101.67(1)
V, Å^3	12498(1)	6367.3(6)	6323.5(6)
Z	4	4	4
D(calcd), mg/m^3	1.579	1.563	1.590
cryst size, mm^3	0.38 × 0.23 × 0.19	0.19 × 0.15 × 0.15	0.10 × 0.08 × 0.06
T, °C	−123	−73	−73
radiation (λ, Å)	Mo Kα (0.71073)	Mo Kα (0.71073)	Mo Kα (0.71073)
μ, mm^{-1}	2.731	2.995	3.351
max and min transm	0.6249 and 0.4234	0.6622 and 0.6000	0.8243 and 0.7305
scan mode	ω at 55/−55	ω at 55/−55	ω at 55/−55
2θ limits, deg	5.52−50.04	5.18−50.06	5.20−54.98
$\pm h$	32	−18, 17	19
$\pm k$	20	18	20
$\pm l$	32	32	−35, 34
no. reflns measd	74253	40178	48890
no. unique reflns	22009	11232	14501
restraints	0	0	0
no. variables	1408	676	676
R1 [b] [$I > 2\sigma(I)$]	0.0554	0.0409	0.0385
wR2 [c] (all data)	0.1361	0.1088	0.1059
R_{int}	0.0636	0.0582	0.0539
GOF	1.066	1.012	1.007

[a] For Ln = Gd, **3**, see Cambridge database CCDC-184355. [b] $R1 = \sum||F_o| - |F_c|/\sum|F_o||$. [c] $wR2 = \{\sum w(F_o^2 - F_c^2)^2/w(F_o^2)^2\}^{1/2}$.

A, B, and C (Figure 1a−c), is obtained. All products are 1-D infinite arrays in the solid state, and the extended structures are supported by Ln−NC−M bridges. *cis*-Cyanide and *trans*-cyanide linkages create diamond (Ln_2M_2; types A and C) and hexagonal (Ln_4M_4; type B) shaped cores. Reactions of $LnCl_3$ and $K_2[M(CN)_4]$ in 1:2 ratios generate 2-D sheetlike arrays with larger hexagonal Ln_6M_6 units (Figure 1d). Type B complexes have been introduced onto the surface of an oxide support (sol−gel titania and on silica), and the structural features are maintained on the basis of IR spectra of the complexes on oxide supports that are identical to the spectra of bulk complexes. The heterometallic precursor can then be converted to catalytic nanoparticles, which show enhanced activity and selectivity over the pure noble transition metal catalyst in the reduction of NO_x,[3d] the selective vapor phase hydrogenation of phenol to cyclohexanone,[3e,f] and the hydrodechlorination of chlorobenzenes.[3g]

Group 10 transition metal(II) cyanides, in general, possess square planar coordination geometries. This constraint limits the variety of Ln−M extended structures. On the other hand, the coordination number of the group 11 metal Cu(I) is variable, and 2-, 3-, and 4-coordinate Cu atoms give rise to linear, planar, and tetrahedral geometries, respectively. Therefore, Cu(I) cyanides offer a more diverse assortment of structural features[5] compared to their group 10 counterparts.

In a preliminary report,[6] we described results from initial studies of Ln−Cu(I) cyanides. It was determined that the reactions of $GdCl_3$ with $K[Cu(CN)_2]$ and $GdCl_3$ with KCN plus CuCN give remarkably different products. Two distinct extended arrays, the 3-D ionic inclusion complex $\{[Gd(DMF)_8][Cu_6(CN)_9]{\cdot}2DMF\}_\infty$ in the first case and the 2-D layer complex $\{Gd_2(DMF)_8Cu_4(CN)_{10}\}_\infty$ in the second case, were isolated. The structural motifs (overall structures and building blocks) are quite unusual considering that they do not resemble the structures of Ln−M(group 10) cyanides or other M−Cu systems. The formation of the two Gd−Cu(I) complexes is contingent upon the synthetic procedure. In view of the unique structural aspects of the Gd−Cu systems,

(5) (a) Chesnot, D. J.; Kusnetaow, A.; Zubieta, J. *J. Chem. Soc., Dalton Trans.* **1998**, 4081−4084. (b) Nishikiori, S.; Iwamoto, T. *J. Chem. Soc., Chem. Commun.* **1993**, 1555−1556. (c) Chesnot, D. J.; Zubieta, J. *Chem. Commun.* **1998**, 1707−1708. (d) Bowmaker, G. A.; Hartl, H.; Urban, V. *Inorg. Chem.* **2000**, *39*, 4548−4554. (e) Zhao, Y.; Hong, M.; Su, W.; Zhou Z.; Chan, A. *J. Chem. Soc., Dalton Trans.* **2000**, 1685−1686. (f) Heller, M.; Sheldrick, W. S. *Z. Anorg. Allg. Chem.* **2001**, *627*, 569−571. (g) Escorihuela, I.; Falvello, L. R.; Tomas, M. *Inorg. Chem.* **2001**, *40*, 636−640. (h) Inoue, M. B.; Inoue, M.; Machi, L.; Brown, F.; Fermando, Q. *Inorg. Chim. Acta* **1995**, *230*, 145−151. (i) Cromer, D. T.; Larson, A. C.; Roof, R. B. *Acta Crystallogr.* **1966**, *20*, 279−282. (j) Kildea, J. D.; Skelton, B. W.; White, A. H. *Aust. J. Chem.* **1985**, *38*, 1329−1334. (k) Hoskins, B. F.; Robson, R. *J. Am. Chem. Soc.* **1990**, *112*, 1546−1554.

(6) Liu, S.; Meyers, E.; Shore, S. G. *Angew. Chem., Int. Ed.* **2002**, *41*, 3609−3611.

Table 2. Selected Bond Lengths (Å) and Bond Angles (deg) for **1**, **2**, **3**, and **4**

compound **1**		compound **2**		compound **3**		compound **4**	
La(1)−O(11)	2.639(4)						
La(2)−O(21)	2.614(4)						
La−O(av)[a]	2.532	Eu(1)−O(av)[a]	2.386	Gd(1)−O(av)[a]	2.377	Er(1)−O(av)[a]	2.334
Cu(1)−N(1a)	1.934(8)	Cu(1)−C(6)	1.880(5)	Cu(1)−C(94)	1.894(5)	Cu(1)−C(9c)#1	1.888(5)
Cu(1)−N(1b)	1.919(7)	Cu(1)−C(8)	1.890(6)	Cu(1)−C(97)	1.894(6)	Cu(1)−N(9e)	1.931(5)
Cu(1)−N(1q)#1	1.957(8)	Cu(1)−N(1)	1.957(6)	Cu(1)−N(96)	1.951(6)	Cu(1)−N(9a)#2	1.943(4)
Cu(2)−C(1a)	1.920(7)	Cu(2)−C(1)	1.899(6)	Cu(2)−C(95)	1.886(6)	Cu(2)−C(9b)#3	1.888(5)
Cu(2)−C(1c)	1.901(7)	Cu(2)−C(2)	1.894(5)	Cu(2)−N(93)	1.952(5)	Cu(2)−C(9d)#4	1.899(4)
Cu(2)−N(1d)	1.914(7)	Cu(2)−N(3)	1.950(6)	Cu(2)−N(94)	1.960(6)	Cu(2)−N(9g)	1.886(6)
C(1a)−N(1a)	1.173(8)	C(1)−N(1)	1.148(6)	C(91)−N(91)#3	1.150(7)	C(9a)−N(9a)	1.158(6)
C(1b)−N(1b)	1.166(8)	C(2)−N(2)	1.155(6)	C(92)−N(92)#5	1.168(7)	C(9b)−N(9b)	1.162(6)
O(11)La(1)O(12)	64.6(1)	O(11)Eu(1)O(12)	77.8(2)	O(1)Gd(1)O(2)	70.9(1)	O(1)Er(1)O(2)	83.1(1)
O(11)La(1)O(13)	71.9(1)	O(11)Eu(1)O(13)	73.0(1)	O(1)Gd(1)O(3)	72.3(1)	O(1)Er(1)O(3)	71.5(1)
O(11)La(1)O(17)	70.9(1)	O(11)Eu(1)O(16)	76.1(1)	O(1)Gd(1)O(7)	73.0(1)	O(1)Er(1)O(7)	74.2(1)
O(11)La(1)O(18)	67.2(1)	O(11)Eu(1)O(18)	82.7(1)	O(1)Gd(1)O(8)	78.7(1)	O(1)Er(1)O(8)	73.5(1)
N(1a)Cu(1)N(1q)	119.2(3)	C(6)Cu(1)C(8)	122.9(2)	C(94)Cu(1)C(97)	119.9(2)	C(9c)Cu(1)N(9e)	123.1(2)
N(1b)Cu(1)N(1a)	]117.6(3)	C(6)Cu(1)N(1)	114.5(2)	C(94)Cu(1)N(96)	116.6(2)	C(9c)Cu(1)N(9a)	122.5(2)
N(1b)Cu(1)N(1q)	123.0(3)	C(8)Cu(1)N(1)	122.6(2)	C(97)Cu(1)N(96)	123.3(2)	N(9e)Cu(1)N(9a)	114.4(2)
C(1a)Cu(2)C(1c)	113.5(3)	C(1)Cu(2)C(2)	120.4(2)	C(95)Cu(2)N(93)	123.9(2)	C(9b)Cu(2)C(9d)	128.4(2)
C(1a)Cu(2)N(1d)	130.8(3)	C(2)Cu(2)N(3)	116.0(2)	C(95)Cu(2)N(94)	125.9(2)	C(9b)Cu(2)N(9g)	119.8(2)
N(1d)Cu(2)C(1a)	115.0(3)	C(1)Cu(2)N(3)	123.4(2)	N(93)Cu(2)N(94)	110.1(2)	C(9d)Cu(2)N(9g)	111.8(2)

[a] La−O(av) is the average distance from all of eight equatorial oxygen atoms O12−O19 and O22−O29, while capping oxygen atoms (O11 and O21) are not included. Other Ln−O(av) distances are from the averages of O11−O18.

it was of interest to ascertain if these synthetic methodologies could be generalized to other Ln−Cu combinations.

Results and Discussion

Inclusion Complexes Formed from Three-Component One-Step Reactions. (A) {[La(DMF)$_9$]$_2$[Cu$_{12}$(CN)$_{18}$]·2DMF}$_\infty$. The simple three-component metathesis reaction involving $LaCl_3$, CuCN, and KCN in DMF (eq 3) generates a 3-D extended, inclusion complex {[La(DMF)$_9$]$_2$[Cu$_{12}$(CN)$_{18}$]·2DMF}$_\infty$ (**1**) after the precipitation of KCl.

$$2LaCl_3 + 12CuCN + 6KCN \xrightarrow[-6KCl]{DMF} \{[La(DMF)_9]_2[Cu_{12}(CN)_{18}]\cdot 2DMF\}_\infty \quad (3)$$

The formation of compound **1** appears to be independent of the ratio of reactants. It was obtained as the sole product over a range of reaction ratios ($LaCl_3$/CuCN/KCN; 1:*n*:3; *n* = 3, 6, 12). Crystals of **1**, grown from DMF solution, are pale brown, almost colorless, while powders are white. Once formed, the crystals are not soluble in DMF or water.

The structure of **1** was determined by single-crystal X-ray diffraction analysis. Crystallographic data and selected bond lengths and bond angles are listed in Tables 1 and 2. Its structure (Figure 2) consists of a three-dimensional extended anionic lattice of composition {[Cu$_{12}$(CN)$_{18}$]$^{6-}$}$_\infty$ (Figure 2a) which contains "pockets" that serve as hosts in sequestering a guest [La(DMF)$_9$]$^{3+}$ cation and one free DMF molecule in each pocket (Figure 2b). The 9-coordinate La(III) in the [La(DMF)$_9$]$^{3+}$ cation has monocapped square antiprismatic geometry (Figure 3). This coordination geometry is also observed for Ce(III) atoms in the type C compound, {(DMF)$_{12}$Ce$_2$[Ni(CN)$_4$]$_3$}$_\infty$ ([Ce(DMF)$_6$(NC−)$_3$]$^{3+}$).[4b] The La−O(square antiprism) bonds range from 2.472(4) to 2.584(4) Å, and they are shorter than the La−O(capping) bonds (av, 2.627 Å). Apparently, the [La(DMF)$_9$]$^{3+}$ cation is the first example of a monocapped square antiprismatic geometry for a nine-coordinate homoleptic La cation.[7,8] On the other hand, the only nine-coordinate homoleptic lanthanum cation [La(H$_2$O)$_9$]$^{3+}$ is of higher symmetry, tricapped trigonal prismatic.[7]

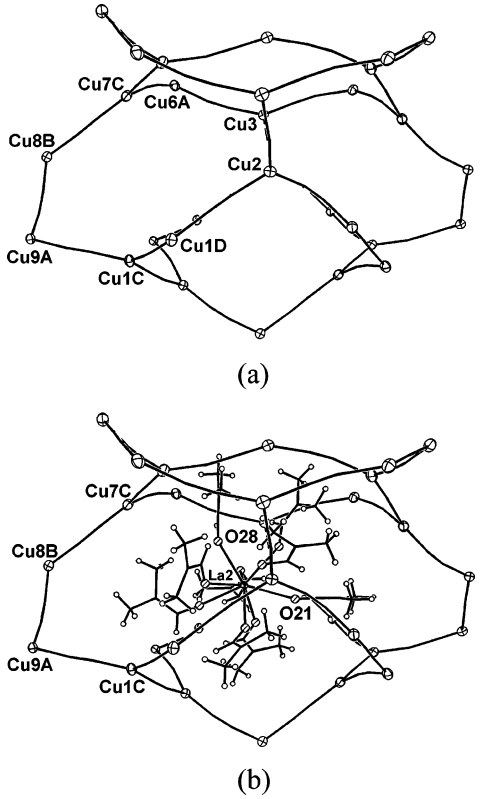

Figure 2. Structure of 1 showing (a) one pocket of the {[Cu$_{12}$(CN)$_{18}$]$^{6-}$}$_\infty$ anionic lattice and (b) a sequestered cation and one free DMF molecule inside the pocket. Carbon and nitrogen atoms are drawn as sticks.

The anionic lattice of **1** is built up of CN$^-$ linkages between Cu atoms. Three cyano groups are coordinated to each Cu in a distorted trigonal planar arrangement. The C−Cu−C and N−Cu−C angles vary from 107.9(2)° to 140.9(3)°.

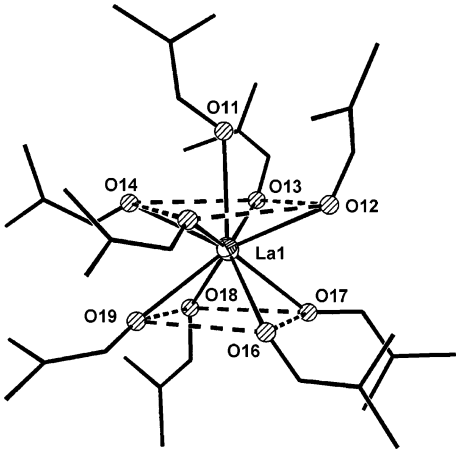

Figure 3. Structures of $\{[La(DMF)_9]_2[Cu_{12}(CN)_{18}]\cdot 2DMF\}_\infty$ (**1**) showing the La(III) coordination geometry. Carbon and nitrogen atoms of DMF ligands are drawn as sticks, and hydrogen atoms are omitted for clarity.

The substructure of the anionic network is a twisted "eight"-membered ring (eight Cu atoms). Five of these eight-membered rings, two ten-membered rings, and one twelve-membered ring couple to create irregular-shaped pockets (30 Cu atoms, 36 cyanide ligands; Cu, C and N atoms are shared between the rings; Figure 2a). Each pocket contains a sequestered $[La(DMF)_9]^{3+}$ cation and one free DMF molecule (Figure 2b). Even though the pocket is irregular, it still follows Euler's rule for polyhedra ($V_{vertexes} = 30$, $E_{edges} = 36$, $F_{faces} = 8$; $V - E + F = 2$).[9] There are 14 neighboring pockets around each enclosure. The cation is truly encapsulated within the anionic cage since the largest pocket window (8.42 Å × 11.71 Å) is smaller than the width (14.72 Å) of the cation.[10] Even though the volume of the cavity is large which would allow for some movement of the La^{3+}, electrostatic interaction between the cation and the anionic pocket, plus the smaller size of the pocket windows compared to the size of the solvated cation, inhibits the cation from leaving the pocket. However, the windows are sufficiently large to allow migration of the free DMF molecules. Close examination of the free solvent molecule reveals that the carbonyl oxygen is directed toward the $[La(DMF)_9]^{3+}$ cation ((free DMF)C═O···H−C(coordinated DMF) weak interactions, 2.2−3.1 Å). This possibly suggests exchange between the free and coordinating solvent molecules. The DMF molecules can be partially removed under vacuum.

Table 3. Crystallographic Data for $\{Ln(DMF)_4Cu_2(CN)_5\}\cdot$(Ln = La, **5**; Er, **7**) and $\{K(DMF)_2Cu(CN)_2\}_\infty$, **8**[a]

	5	**7**	**8**
empirical formula	$C_{34}H_{56}Cu_4La_2N_{18}O_8$	$C_{34}H_{56}Cu_4Er_2N_{18}O_8$	$C_8H_{14}CuKN_4O_2$
fw	1376.94	1433.64	300.87
cryst syst	monoclinic	monoclinic	orthorhombic
space group	$P2_1$	$P2_1$	*Pbca*
a, Å	9.186(1)	9.035(1)	7.665(1)
b, Å	18.198(1)	17.937(1)	18.450(1)
c, Å	16.643(1)	16.320(1)	18.681(1)
β, deg	95.94(1)	95.17(1)	
V, Å^3	2767.1(4)	2634.2(4)	2642.0(4)
Z	2	2	8
ρ(calcd), mg/m^3	1.828	1.808	1.513
cryst size, mm^3	0.27 × 0.19 × 0.15	0.23 × 0.19 × 0.15	0.15 × 0.12 × 0.06
T, °C	−33	−73	−73
radiation (λ, Å)	Mo Kα (0.71073)	Mo Kα (0.71073)	Mo Kα (0.71073)
μ, mm^{-1}	3.151	4.795	1.960
max and min transm	0.6493 and 0.4833	0.5332 and 0.4051	0.8914 and 0.7175
scan mode	*T* at 55/−55	*T* at 55/−55	*T* at 55/−55
2θ limits, deg	4.86−54.92	3.38−50.04	4.92−50.04
±*h*	11	10	9
±*k*	23	21	21
±*l*	21	19	22
no. reflns measd	23285	42762	13942
no. unique reflns	12632	9233	2328
restraints	1	1	0
no. variables	596	596	145
R1 [b] [$I > 2\sigma(I)$]	0.0324	0.0377	0.0463
wR2 [c] (all data)	0.0811	0.0827	0.1345
R_{int}	0.0350	0.0687	0.0489
GOF	1.019	1.032	1.048

[a] For Ln = Gd, **6**, see Cambridge database CCDC-184356. [b] $R1 = \sum||F_o| - |F_c|/\sum|F_o||$. [c] $wR2 = \{\sum w(F_o^2 - F_c^2)^2/w(F_o^2)^2\}^{1/2}$.

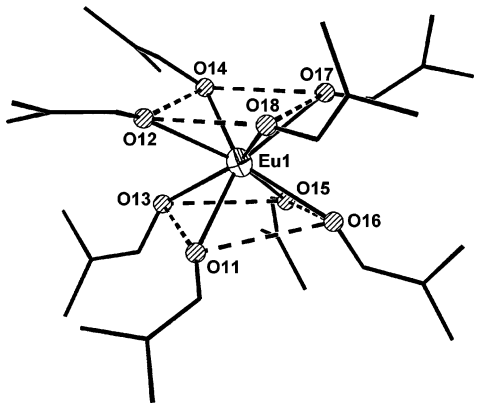

Figure 4. Structures of $\{[Eu(DMF)_8][Cu_6(CN)_9]\cdot 2DMF\}_\infty$ (**2**) showing the Eu(III) coordination geometry. Carbon and nitrogen atoms of DMF ligands are drawn as sticks, and hydrogen atoms are omitted for clarity.

Each Cu is trigonally coordinated to cyanide ligands. It is difficult to distinguish between C and N atoms due to possible linkage isomerism because the cyanide is bridging two like metals (Cu−CN−Cu or Cu−NC−Cu). When the cyanide ion bridges a lanthanide metal and a transition metal no linkage isomerism (Ln−NC−M′, Ln−CN−M′) is observed in the complexes since the soft Lewis basic carbon end of $[CN]^-$ prefers the softer Lewis acidic transition metal ion. When there is only one transition metal in the network, it is very difficult to determine which atom is C or N. This uncertainty is present in several published works which

(7) (a) Steed, J. W.; Johnson, C. P.; Barns, C. L.; Juneja, R. K.; Atwood, J. L.; Reilly, S.; Hollis, R. L.; Smith, P. H.; Clark, D. L. *J. Am. Chem. Soc.* **1995**, *117*, 11426−11433. (b) Faithfull, D. L.; Harrowfield, J. M.; Skelton, B. W.; Third, K.; White, A. H. *Aust. J. Chem.* **1992**, *45*, 583−594. (c) Chatterjee, A.; Maslen, E. N.; Watson, K. J. *Acta Crystallogr. B: Struct. Sci.* **1988**, *44*, 381−386. (d) Gerkin, R. E.; Reppart, W. J. *Acta Crystallogr. C: Cryst. Struct. Commun.* **1984**, *40*, 781−786. (e) Harrowfield, J. M.; Kepert, D. L.; Patrick, J. M.; White, A. H. *Aust. J. Chem.* **1983**, *36*, 483−492.

(8) (a) Chen, L.; Wu, X.; Gao, X.; Zhang, W.; Lin, P. *J. Chem. Soc., Dalton Trans.* **1999**, 4303−4307. (b) Chen, L.; Wu, X.; Lin, P. *J. Chem. Crystallogr.* **1999**, *29*, 629−633.

(9) Meserve, B. E. *Fundamental Concepts of Geometry*; Dover Publications: 1983; p 301.

(10) (a) The dimensions are measured through the atomic centers in Shelx software, and then, van der Waals radii were taken into account. (b) The van der Waals radii of H (1.20 Å) and Cu(I) (0.96 Å) were obtained from www.webelements.com/. For more detailed calculation, please see Supporting Information.

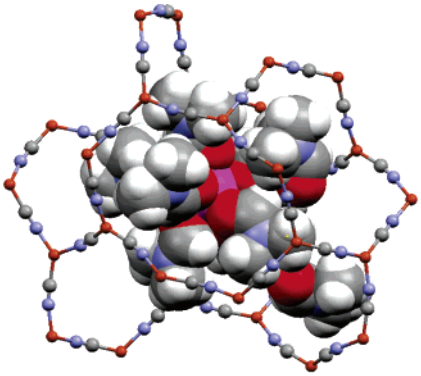

Figure 5. Structure of **2** showing the encapsulated $[Eu(DMF)_8]^{3+}$ cation and two free DMF molecules in the pocket.

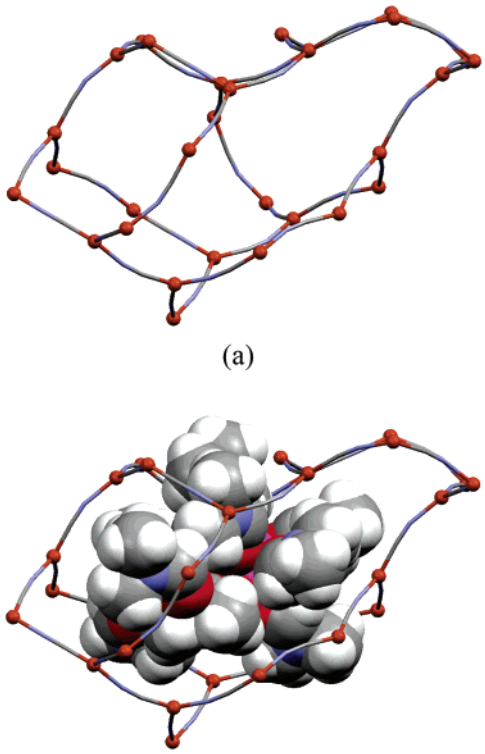

Figure 6. Structures of $\{[Er(DMF)_8][Cu_6(CN)_9]\cdot 2DMF\}_\infty$ (**4**). (a) One pocket of the $\{[Cu_6(CN)_9]^{6-}\}_\infty$ anionic lattice. Carbon and nitrogen atoms are drawn as sticks. (b) A sequestered cation and two free DMF molecules (drawn as spacefill) inside the pocket.

designate CN bridges as X atoms.[11] In this paper, we have attempted to resolve the problem in the following way. All of the CN ligand atoms were assigned as nitrogen atoms, and then their occupancies were refined. The higher occupancy in a ligand atom (90−100%) is assigned to N, and a lower occupancy (75−90%) is assigned to C, consistent with the fact that the atomic number of nitrogen is 17% larger than carbon. The results indicate that there is no obvious random disorder of CN units.

(11) See, for example: (a) Colacio, E.; Dominguez-Vera, J. M.; Lloret, F.; Sanchez, J. M. M.; Kivekas, R.; Rodriguez, A.; Sillanpaa, R. *Inorg. Chem.* **2003**, *42*, 4209−4214. (b) Colacio, E.; Kivekas, R.; Lloret, F.; Sunberg, M.; Suarez-Vera, J.; Bardaji, M.; Laguna, A. *Inorg. Chem.* **2002**, *41*, 5141−5149.

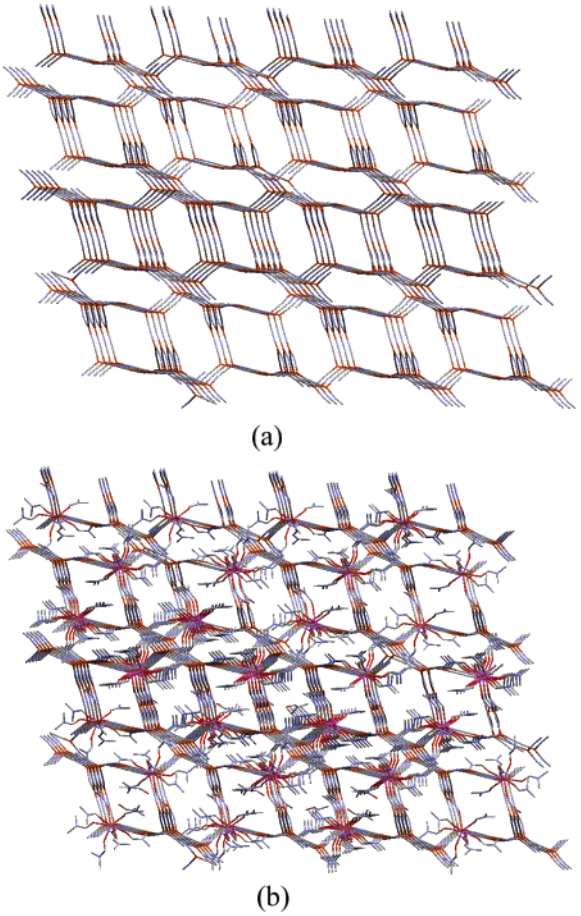

Figure 7. Structure of **2** showing (a) the $\{[Cu_{12}(CN)_{18}]^{6-}\}_\infty$ anionic lattice and (b) sequestered cations and free DMF molecules inside the pockets of the lattice.

(B) $\{[Ln(DMF)_8][Cu_6(CN)_9]\cdot 2DMF\}_\infty$ (Ln = Eu, Gd, Er). When smaller lanthanide cations (Ln = Eu, Gd, Er) are employed under the same reaction conditions as eq 3, similar inclusion complexes, **2**, **3**, and **4**, are obtained (eq 4). Single-crystal X-ray analyses reveal these three complexes to be isostructural.

$$LnCl_3 + 6CuCN + 3KCN \xrightarrow[-3KCl]{DMF} \{[Ln(DMF)_8][Cu_6(CN)_9]\cdot 2DMF\}_\infty \quad (4)$$
$$Ln = Eu, \mathbf{2}; Ln = Gd, \mathbf{3}; Ln = Er, \mathbf{4}$$

Crystallographic data and selected bond lengths and bond angles of **2**, **3**, and **4** are listed in Tables 1 and 2. The asymmetric units of these complexes consist of one $[Ln(DMF)_8]^{3+}$ cation, two free DMF solvent molecules, and the counterion, $[Cu_6(CN)_9]^{3-}$, which is about half the size of the formula of complex **1**.

The eight-coordination geometries of the lanthanide centers in $[Ln(DMF)_8]^{3+}$ are square-antiprismatic (Figure 4). There are two DMF molecules encapsulated with each $[Ln(DMF)_8]^{3+}$ (Figures 5 and 6b). The C−Cu−C and N−Cu−C angles vary from 105.5(2)° to 135.1(2)° in all of the three isostructural compounds, and they differ from those in **1**. The anionic pockets (Figure 6a) differ slightly in shape compared to those in the network for compounds **2**, **3**, and **4**, respectively. The lanthanide cation cannot leave the pocket

Table 4. Selected Bond Lengths (Å) and Bond Angles (deg) for **5**, **6**, **7**, and **8**

compound **5**		compound **6**		compound **7**		compound **8**	
La(1)−O(av)	2.489	Gd(1)−O(av)	2.401	Er(1)−O(av)	2.333		
La(1)−N(av)	2.618	Gd(1)−N(av)	2.498	Er(1)−N(av)	2.439		
Cu(1)−C(1)	1.920(6)	Cu(1)−C(1a)	1.919(11)	Cu(1)−C(1g)	1.930(13)	Cu(1)−C(11)	1.900(5)
Cu(1)−C(2)	1.931(7)	Cu(1)−C(1b)	1.934(12)	Cu(1)−C(1i)	1.939(14)	Cu(1)−C(12)	1.922(5)
Cu(1)−C(3)	1.946(6)	Cu(1)−N(1)	1.973(12)	Cu(1)−C(1j)	1.954(11)	Cu(1)−N(12)	1.963(5)
Cu(2)−N(3)	1.973(6)	Cu(2)−C(1)	1.920(11)	Cu(2)−C(1b)	1.925(15)		
Cu(2)−C(4)	1.925(6)	Cu(2)−C(2a)	1.901(12)	Cu(2)−C(1c)	1.938(14)		
Cu(2)−C(5)	1.920(6)	Cu(2)−C(2b)	1.938(12)	Cu(2)−N(1j)	1.978(14)		
C(1)−N(1)	1.147(9)	C(1)−N(1)	1.149(13)	C(1a)−N(1a)	1.143(15)	C(11)−N(11)	1.145(6)
C(2)−N(2)	1.151(8)	C(1a)−N(1a)	1.136(12)	C(1b)−N(1b)	1.153(17)	C(12)−N(12)	1.159(6)
N(10)#1−La(1)−N(5)#2	76.8(2)	N(1A)−Gd(1)−N(4A)#3	76.7(3)	N(1A)−Er(1)−N(1G)	76.5(4)		
N(10)#1−La(1)−N(4)	84.3(2)	N(1A)−Gd(1)−N(4B)#2	83.6(3)	N(1A)−Er(1)−N(1I)	83.8(4)		
N(7)−La(1)−N(4)	92.2(2)	N(2A)#1−Gd(1)−N(4B)#2	92.7(3)	N(1I)−Er(1)−N(1H)	93.0(4)		
N(7)−La(1)−N(5)#2	87.5(2)	N(2A)#1−Gd(1)−N(4A)#3	88.0(3)	N(1H)−Er(1)−N(1G)	87.0(4)		
C(1)Cu(1)C(2)	121.2(3)	C(2a)Cu(2)C(2b)	125.3(5)	C(1g)Cu(1)C(1i)	127.9(5)	C(11)Cu(1)N(12)	127.8(2)
C(2)Cu(1)C(3)	119.6(3)	C(2a)Cu(2)C(1)	119.7(4)	C(1g)Cu(1)C(1j)	116.8(5)	C(11)Cu(1)C(12)	124.7(2)
C(1)Cu(1)C(3)	118.4(3)	C(1)Cu(2)C(2b)	114.9(4)	C(1i)Cu(1)C(1j)	115.2(5)	C(12)Cu(1)N(12)	107.5(2)
C(4)Cu(2)C(5)	126.2(3)	C(1a)Cu(1)C(1b)	132.9(4)	C(1b)Cu(2)C(1c)	120.6(5)		
C(5)Cu(2)N(3)	117.7(2)	C(1a)Cu(1)N(1)	113.6(4)	C(1c)Cu(2)N(ij)	119.5(5)		
C(4)Cu(2)N(3)	116.0(2)	C(1b)Cu(1)N(1)	113.1(4)	C(1b)Cu(2)N(ij)	119.0(5)		

due to the electrostatic interactions, and the openings of the pocket are smaller than the size of lanthanide cations coordinated to DMF ligands (sizes of the lanthanide cations: Eu, 15.09 Å; Gd, 15.08 Å; Er, 14.96 Å).[10] Similar to **1**, each pocket of **2**, **3**, and **4** has 30 three-coordinate copper atoms connected to 36 cyanide linkages, and it is irregular in shape. The three-dimensional network is shown in Figure 7.

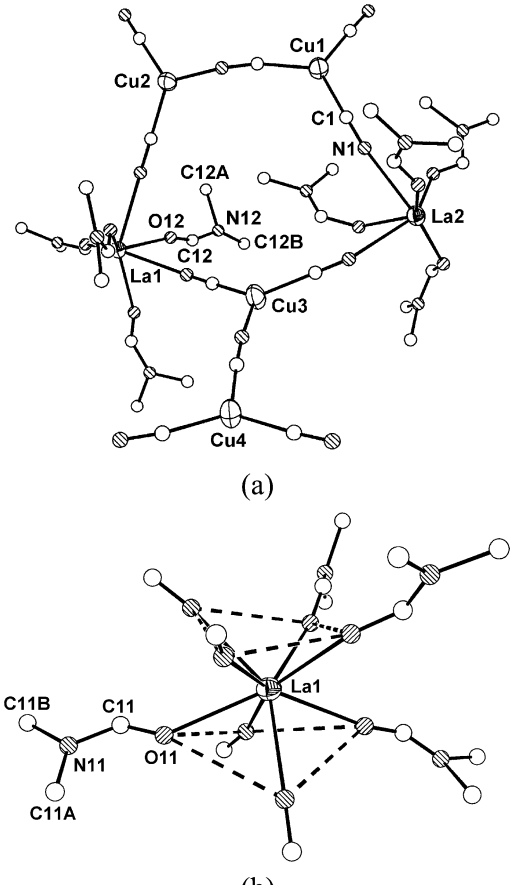

Figure 8. Structure of $\{La(DMF)_4Cu_2(CN)_5\}_\infty$ (**5**) showing (a) the asymmetric unit and (b) the La(III) coordination geometry. Hydrogen atoms are omitted for clarity.

There are no significant differences between the anionic three-dimensional networks of **2**, **3**, **4**, and **1**. In **2**, **3**, and **4**, the cations are eight-coordinate and there are two encapsulated solvent molecules per anionic cage, but in **1** the cation is nine-coordinate and there is one free DMF molecule in each pocket. We believe that encapsulation of the cations occurs through build-up of the anionic structure, by the linkage of cyanide to Cu(I), around the cations due to charge compensation. The "windows" of the anionic pockets appear to be sufficiently large for the solvent molecules to diffuse into the pockets. To our knowledge, these complexes are the first examples of encapsulated lanthanide cations. The anionic network itself is also unique because the three-dimensional arrangement of three-coordinate Cu(I) atoms has not been previously reported. However, a three-dimensional array consisting of four-coordinate copper cyanide anionic centers with included $[Cu(en)_2H_2O]^{2+}$ cations in large lattice vacancies is known.[12a] Similarly, neutral, tetrahedral cadmium cyanide networks with encaged neutral small molecules are reported.[12b,c] Two- and three-coordinate Cu(I)−cyanide systems are known to have 1- and 2-dimensional structures that also incorporate other ligands besides cyanide.[5]

Our original procedure for preparing the Er encapsulation complex was modified to employ CuCl in place of CuCN (eq 5). The yield of **4** was equivalent to that obtained from the synthesis in eq 4. The reaction time is also slow because of the low solubility of CuCl in DMF.

$$ErCl_3 + 6CuCl + 9KCN \xrightarrow[-9KCl]{DMF} \{[Er(DMF)_8][Cu_6(CN)_9]\cdot 2DMF\}_\infty \quad (5)$$

Two Step Reaction. Formation of Layered Structures. As pointed out in the Introduction, our earlier syntheses of cyanide-bridged lanthanide−group 10 transition metal complexes produced the same product from two different

(12) (a) Williams, R. J.; Larson, A. C.; Cromer, D. T. *Acta Crystallogr.* **1972**, *B28*, 858−864. (b) Kitazawa, T.; Nishikiori, S.; Yamagishi, A.; Kuroda, R.; Iwamoto, T. *J. Chem. Soc., Chem. Commun.* **1992**, 413−415. (c) Kitazawa, T.; Nishikiori, S.; Kuroda, R.; Iwamoto, T. *Chem. Lett.* **1988**, 1729−1732.

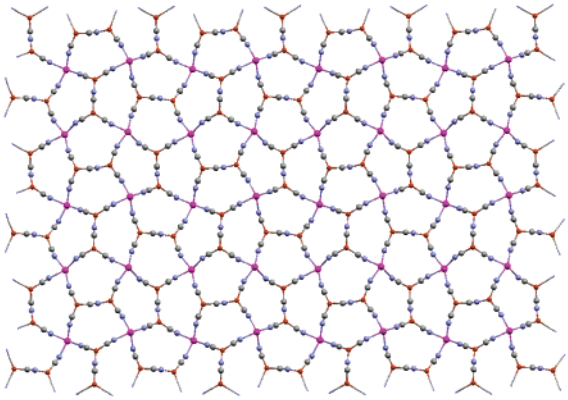

Figure 9. Structure of $\{La(DMF)_4Cu_2(CN)_5\}_\infty$ (**5**) showing a single layer. DMF ligands are omitted for clarity.

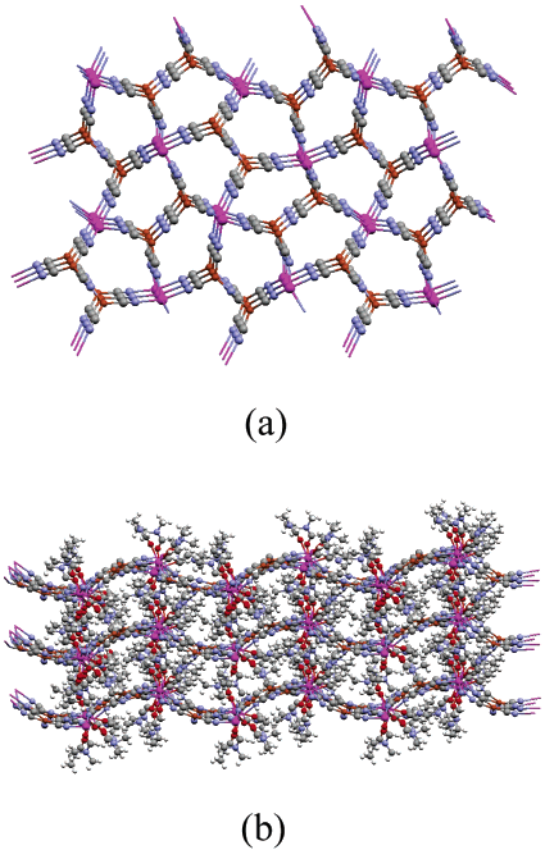

Figure 10. Structure of $\{La(DMF)_4Cu_2(CN)_5\}_\infty$ (**5**) showing the (a) top view and (b) cross-section of three stacked layers. DMF ligands are omitted for clarity in part a.

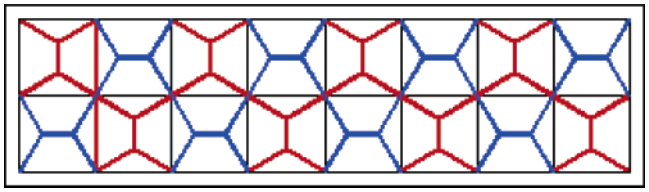

Figure 11. The Cairo tile.

synthetic procedures. One procedure (eq 2) involved the reaction of the three components $LnCl_3$, KCN, and a group 10 dichloride MCl_2, while the other preparative route (eq 1) involved the combination of $LnCl_3$ with a group 10 tetracyanato salt, $K_2[M(CN)_4]$. On the other hand, for Ln−Cu

Scheme 1. Proposed Self-Assembly of the Anionic Network ($\{[Cu_6(CN)_9]^{3-}\}_\infty$) around Ln Cation in **1**−**4**

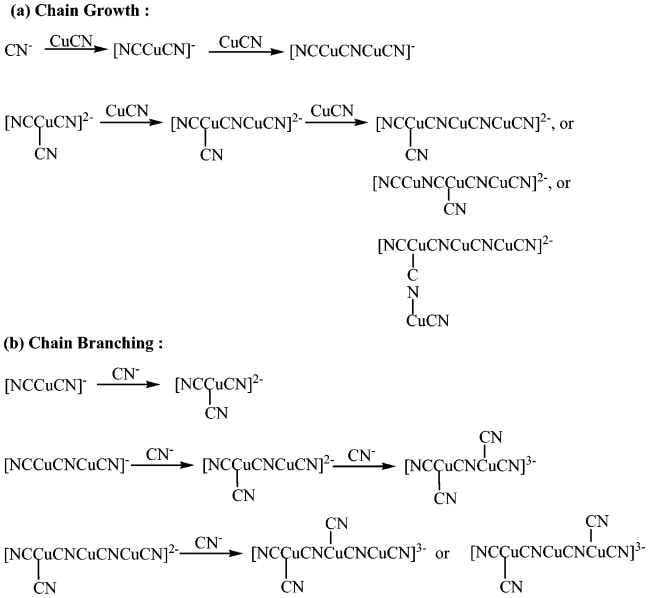

Chart 1

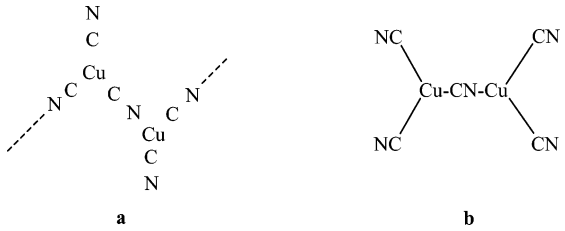

complexes, two procedures analogous to those employed in the preparation of the lanthanide−group 10 metal complexes yield different structural types. The first synthetic procedure (eqs 3 and 4) produces the inclusion complexes **1**−**4**, while the second procedure (eq 6a,b) gives rise to layer structures of a new type, $\{Ln(DMF)_4Cu_2(CN)_5\}_\infty$.

$$CuCN + KCN \xrightarrow{DMF} \{K(DMF)_2Cu(CN)_2\}_\infty \quad (6a)$$

$$2LnCl_3 + 6KCu(CN)_2 \xrightarrow[-6KCl,\ -2CuCN]{DMF} \{(DMF)_8Ln_2\{Cu_4(CN)_{10}\}_\infty \quad (6b)$$

Ln = La, **5**; Gd, **6**; Er, **7**

The first step of the two-step reaction (eq 6a) produces a potassium Cu(I) cyanometalate, which is the analogue of group 10 M(II) metalates. After the reaction, the DMF solvent is removed, and the second step (eq 6b) is initiated by the addition of lanthanide trichloride to a DMF solution of $K[Cu(CN)_2]$.

Colorless crystals of $\{La(DMF)_4Cu_2(CN)_5\}_\infty$, **5**, and $\{Gd(DMF)_4Cu_2(CN)_5\}_\infty$, **6**, and pink crystals of $\{Er(DMF)_4Cu_2(CN)_5\}_\infty$, **7**, are obtained. They are isostructural on the basis of single-crystal X-ray analyses. Crystallographic data and selected bond lengths and bond angles are listed in Tables 3 and 4. The complexes **5**, **6**, and **7** have layer structures, examples of which are shown in Figures 8−10. Since these complexes are isostructural, only **5** is discussed here. Figure 8a shows the asymmetric unit, $\{La(DMF)_4Cu_2(CN)_5\}_2$, of

Scheme 2. Formation of the Layer Structures in **5**−**7**

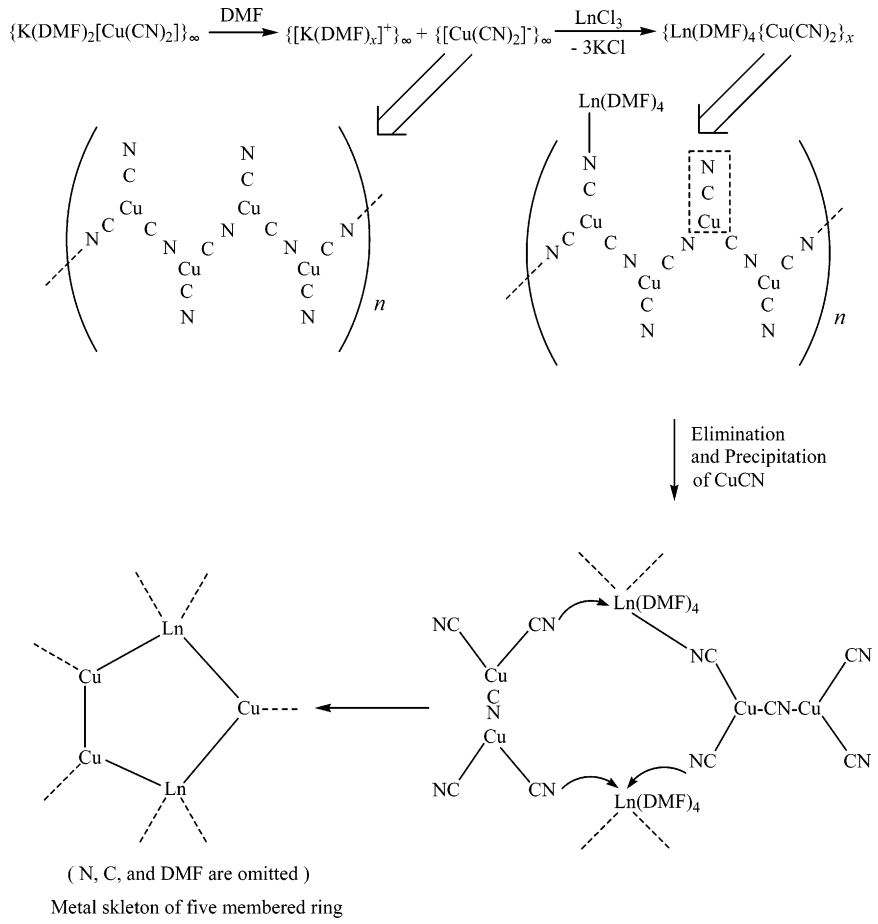

the complex, $\{La(DMF)_4Cu_2(CN)_5\}_\infty$, **5**. Two different cyanide connections are observed in this unit: two Cu(I) atoms are linked through a cyanide bridge, and each Cu(I) atom is linked to two La(III) atoms through cyanide bridges. The La(III) is bonded to four DMF molecules and four bridging cyanide ligands, which leads to a distorted square-antiprismatic coordination geometry (Figure 8b). Each Cu(I) is coordinated to three cyanide ligands. The cyanide bridged La_2Cu_3 five-membered ring is the basic unit that shares common edges and generates the two-dimensional structure (Figure 9). The layers are puckered. Figure 10a,b shows views of three stacked layers with DMF molecules omitted for clarity.

It should be noted that although La is larger than Gd and Er, all three lanthanides are eight-coordinate (square antiprismatic) in **5**, **6**, and **7**. However, in most lanthanide complexes La(III) is nine-coordinate as in the case of **1** except for the stereochemical requirements imposed by bulky ligands.[8] There is no apparent linkage isomerism in the Ln−NC−Cu(I) bridges in these complexes. In the Cu(I)−CN−Cu(I) connections, the C and N atoms were assigned by the same method as was described in the discussion of the encapsulation complexes. Angles for three-coordinate copper(I) vary from 113.9(3)° to 130.6(3)° for **5** (**6**, 113.1(4)−132.9(4)°; **7**, 12.5(5)−133.7(5)°). Although these angles differ significantly from the ideal 120°, the discrepancies are less than those in the inclusion complexes **1**−**4**.

The angles of the pentagonal unit are N(7)−La(1)−N(4) = 92.2(2)°, N(6)−La(2)−N(1) = 84.5(2)°, C(1)−Cu(1)−C(3) = 118.4(3)°, C(4)−Cu(2)−N(3) = 116.0(2)°, and C(7)−Cu(3)−C(6) = 125.0(3)°, respectively, and their sum, 536°, compares well with that for a planar pentagon, 540°. These five-membered rings join to form the puckered sheet structure. Puckering of the sheet occurs where the lanthanide atoms reside, corners with four connections, Figure 9. This five-membered ring building block is unusual compared to other lanthanide−transition metal cyanide-bridged systems. The basic units in lanthanide−group 10 transition metal systems are generally four-membered or six-membered rings.[4]

The first example of a two-dimensional $(5,^3_4)$-network with the five-membered ring basic unit was reported by Zaworotko and co-workers.[13] However, the corners of the pentagon are HMTA ligands and Cu atoms are one the edges of the pentagon. The puckered layer structure is formed through the coordination number of three and four nitrogen atoms of the tetrahedral ligand, HMTA, which is quite different from the structure reported here. In the present case, one small ligand, CN^-, is used in the connections of the pentagon unit; the size of the five-membered ring and the thickness of the layer are much smaller than Zaworotko's. Pentagonal frameworks are combined to form two-dimen-

(13) Moulton, B.; Lu, J.; Zaworotko, M. J. *J. Am. Chem. Soc.* **2001**, *123*, 9224−9225.

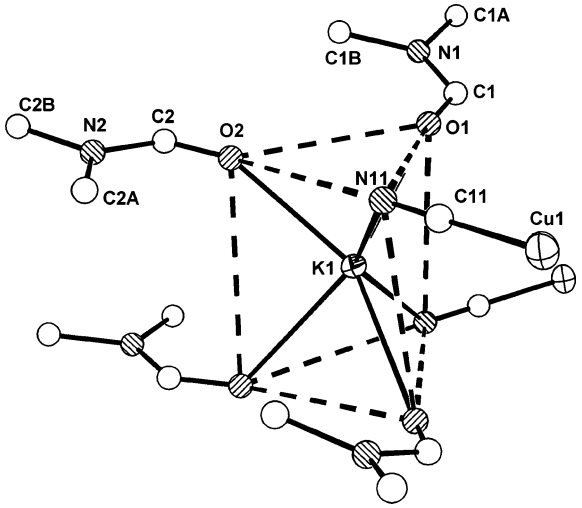

Figure 12. Coordination geometry of K^+ in $\{K(DMF)_2Cu(CN)_2\}_\infty$ (**8**).

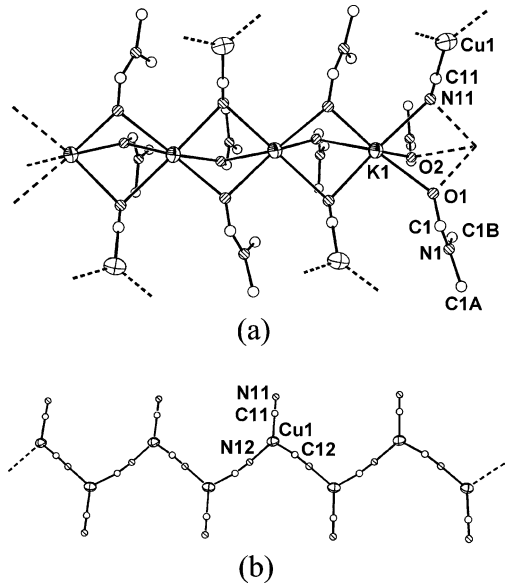

Figure 13. Structures of **8** showing portions of (a) the potassium cationic chain and (b) the $\{[Cu(CN)_2]^-\}_\infty$ anionic chain.

sional structure like Cairo tiling (Figure 11),[14] but the layers are puckered and the pentagons are irregular in shape.

Possible Pathways for the Formation of The Two Structural Types. We are not aware of an experimental approach that can reveal the reaction pathways for the formation of the two different structural types. However, it is of interest to propose reasonable reaction routes based upon the reaction conditions and the relative solubilities of system components observed in this study. The inclusion complexes, **1**−**4**, are prepared from one-step reactions which contain initial reaction mixtures of CuCN, KCN, and $LnCl_3$. On the other hand, the layer complexes, **5**−**7**, are generated from two-step reactions in which CuCN and KCN are first allowed to form $KCu(CN)_2$ and then the $LnCl_3$ is added to the reaction mixture. For the following reasons, we account for the difference in products based on the difference in procedures.

A. Formation of Inclusion Complexes 1−**4.** Among the three reactants, CuCN has the lowest solubility in DMF. The poor solubility of CuCN in DMF results in a low concentration of $K[Cu(CN)_2]$ at any given time, while the more soluble $LnCl_3$ reacts with KCN to precipitate KCl, and to produce the completely solvated lanthanide cation, $[Ln(DMF)_n]^{3+}$ ($n = 8, 9$). Addition of CN^- to the lanthanide cation is restricted by the DMF ligands plus the fact that CN^- readily reacts with CuCN to form soluble species $[Cu(CN)_2]^-$ as CuCN slowly goes into solution. The nucleophilicity of the anion $[Cu(CN)_2]^-$ is not sufficient to displace the DMF ligands from the cation to form Cu−CN−Ln bridges. As more CuCN slowly goes into solution, it reacts with the $[Cu(CN)_2]^-$ anion to give a growing chain, Scheme 1a. Branching of the chain, Scheme 1b, can occur through reaction with CN^-. The combination of these two processes results in the formation of pockets around the cation and chain branching that yields a three-dimensional anionic array, the polymeric anion $\{[Cu_2(CN)_3]^-\}_\infty$. This anion builds up around the solvated lanthanide cations yielding connected pockets that sequester the cations. The slow assembly of the copper−cyanide anionic pocket around the solvated lanthanide cation is due to the limited solubility of the CuCN. The formation of the crystalline inclusion complex requires several weeks, and it is insoluble in DMF and water. Clearly, the self-assembly process continues in solution until solubility is exceeded and then precipitation occurs.

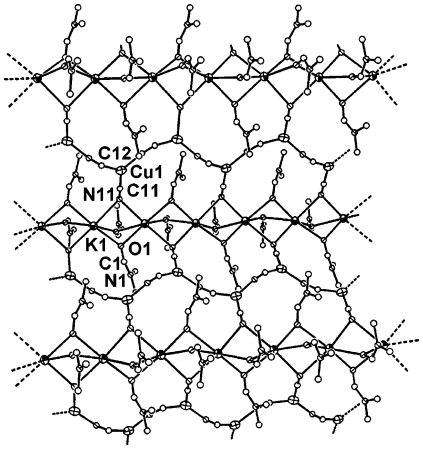

Figure 14. Structure of **8** showing a single layer.

B. Formation of Layer Complexes 5−**7.** By starting with $\{K(DMF)_2Cu(CN)_2\}_\infty$ which is much more soluble in DMF than $LnCl_3$, the anion is available to compete with DMF for coordination to the lanthanide cation as the $LnCl_3$ slowly dissolves. The anion derived from DMF solution, as discussed in the following section, is a one-dimensional chain with the linkages shown in Chart 1a. Four such units and four DMF molecules coordinate to Ln(III) with the elimination and precipitation of one CuCN for every Ln(III) coordinated to the chain. Rupture of the chain occurs at the site of elimination of CuCN. At this point the solution is clear and CuCN and KCl are precipitates that are removed by filtration. Within 24 h, the solution forms a precipitate of the layer structure. During this process five membered rings form that contain two Ln(III) and three Cu(I) atoms bridged by CN^-, Scheme 2. They share common sides with neighboring rings to produce the layer structure.

(14) http://www.counton.org/explorer/morphing/05newfromold.shtml.

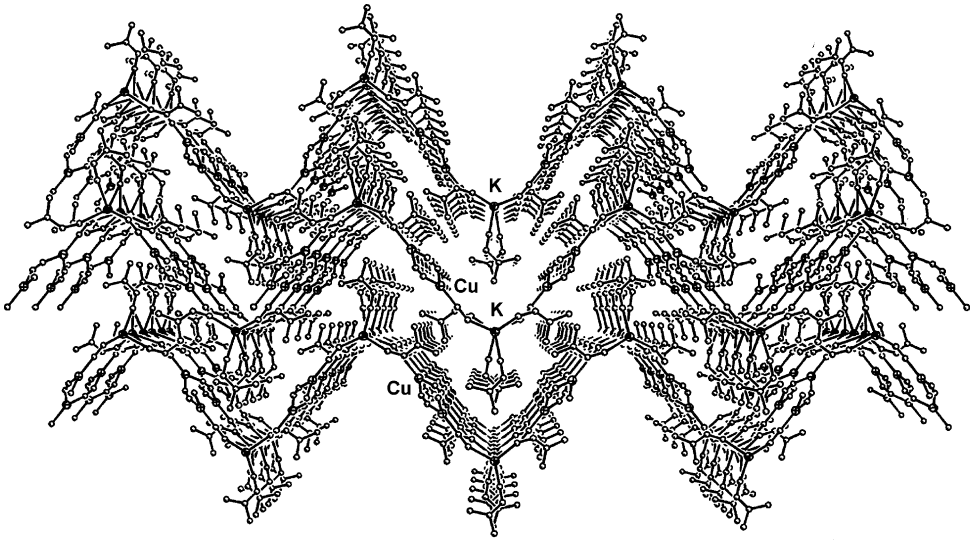

Figure 15. Structure of **8** showing the cross-section of three stacked layers.

The Crystal Structure of $\{K(DMF)_2Cu(CN)_2\}_\infty$. The structure of $KCu(CN)_2$, crystallized from H_2O, was reported in 1957.[15] The main structural feature of this compound is a one-dimensional zigzag anionic chain, $[\{Cu(CN)_2\}_\infty]^{\infty-}$. No solvent ($H_2O$) is in the crystalline material. Since the syntheses of the layer structures **5**−**7** employ $\{K(DMF)_2Cu(CN)_2\}_\infty$ as one of the starting materials, it was of interest to determine the structure of the $[\{Cu(CN)_2\}_\infty]^{\infty-}$ anion when DMF solvent is present. The salt $\{K(DMF)_2Cu(CN)_2\}_\infty$, **8**, was crystallized from DMF. Its structure is shown in Figures 11−14. Crystallographic data and selected bond lengths and bond angles are listed in Tables 3 and 4. As shown in Figure 12, each potassium cation has trigonal prismatic coordination geometry. It is coordinated to four DMF molecules and two cyanides. The potassium ions are linked through DMF double bridges and cyanide double bridges to form an extended cationic chain, Figure 13a. The Cu(I) atoms are three-coordinate, bound to three cyanides. They exist in an extended anionic chain with cyanide bridges, Figure 13b. The nitrogen atoms (N11) of the "terminal" cyanides in the anionic chain bridge the potassium ions and therefore connect cationic chains and anionic chains. These are η^2,μ_3-bridges. The resulting structure is the extended two-dimensional arrangement shown in Figure 14. The layer is puckered, and the stacked layers are shown in Figure 15. The N−K distances, 2.783(4) and 2.830(4) Å, are comparable to those in $[(Me_2PhSi)_3CCuCNK]_4$.[16] However, N−K interactions are weak compared to N−Ln interactions. This is also supported by comparison of bond distances and bond angles in the anionic chain. The distances associated with the terminal cyanide, 1.900(5) Å of Cu(1)−C(11) and 1.145(6) Å for C(11)−N(11), are shorter than those for the bridging cyanide in the anionic chain, 1.922(5) Å for Cu(1)−C(12) and 1.159(6) Å for C(12)−N(12), respectively (Figure 16). On the other hand, the angles between terminal cyanide and bridging cyanide (C(11)−Cu(1)−N(12), 127.8(2)°; C(11)−Cu(1)−C(12), 124.7(2)°) are larger than the angle between bridging cyanides in the anionic chain, C(12)−Cu(1)−N(12), 107.5(2)°.

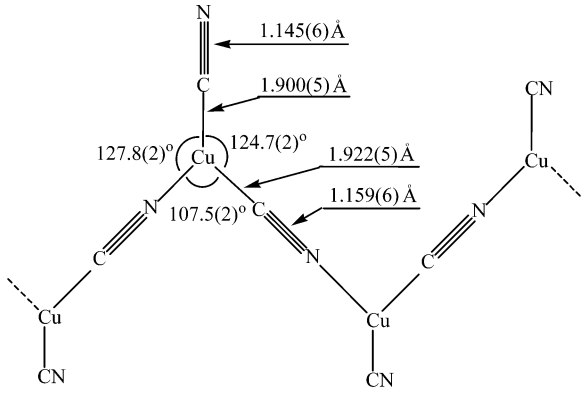

Figure 16. Important bond distances and angles in the anionic copper−cyanide chain of **8**.

IR Spectra. Even though the Cu coordination is always three in the complexes described here, the differences in cyanide bridging connections of the three-dimensional inclusion complexes, **1**−**4**, the two-dimensional layer compounds, **5**−**7**, and $\{K(DMF)_2Cu(CN)_2\}_\infty$, **8**, are obvious. First of all, in the inclusion complexes, all of the cyanide ligands are bridging, coordinated to copper atoms. The solid state IR spectra in the CN stretching region only consist of one broad band 2112 cm^{-1}. Second, there are two different cyanide bridge linkages, Ln−NC−Cu, and Cu−CN−Cu in the layer complexes. However, only one broader stretch is observed probably due to the overlap of two stretches. Two major streches, 2110, and 2089 cm^{-1}, are observed in $\{K(DMF)_2Cu(CN)_2\}_\infty$, **8**.

Experimental Section

All manipulations were carried out on a standard high vacuum line or in a drybox under an atmosphere of dry, pure nitrogen. The purification of dimethylformide (Baker) and the activation of Linde brand molecular sieves (4 Å) are described in a previous publication.[4e] FTIR spectra were recorded on a Mattson Polaris Fourier transform

(15) (a) Cromer, D. T. *J. Phys. Chem.* **1957**, *61*, 1388−1392. (b) Graybeal, J. D.; McKown, G. L. *Inorg. Chem.* **1966**, *5*, 1909−1913.
(16) Eaborn, C.; Hill, M. S.; Hitchcock, P. B.; Smith, J. D. *Organometallics* **2000**, *19*, 5780−5783.

spectrometer with 2 cm^{-1} resolution. All samples were prepared in the drybox. Elemental analyses of materials were performed by Galbraith Laboratories, Inc., Knoxville, TN.

Single-crystal X-ray diffraction data for **1**−**8** were collected on an Enraf−Nonius KappaCCD diffraction system, which employs graphite-monochromated Mo Kα radiation ($\lambda = 0.71073$ Å). Data integration was carried out for Lorentz and polarization effects using Denzo-SMN package (Nonius BV, 1999).[17] Absorption corrections were applied using the SORTAV program[18] provided by MaXus software.[19] The structure was solved by the direct method and refined using the SHELXL-97 (difference electron density calculation, full matrix least-squares refinements) structure solution package.[20] Data merging was performed using the data preparation program supplied by SHELXTL-97. After all non-hydrogen atoms were located and refined anisotropically, hydrogen atoms on DMF molecules were calculated assuming standard CH geometries. Two DMF solvent molecules crystallize with 1 mol of the cation, $[Ln(DMF)_8]^+$, and anionic unit, $[Cu_6(CN)_9]^-$, for **2**, **3**, and **4**. For complex **1**, two DMF solvent molecules cocrystallize with two $[La(DMF)_9]^+$ cations along with the anionic unit, $[Cu_{12}(CN)_{18}]^-$, in the formation of the inclusion complexes.

$\{$**[La(DMF)$_9$]$_2$[Cu$_{12}$(CN)$_{18}$]·2DMF**$\}_\infty$**, 1.** $LaCl_3$ (250 mg, 1.02 mmol), CuCN (274 mg, 3.06 mmol), and KCN (199 mg, 3.06 mmol) in a 1:3:3 ratio were stirred in DMF (ca. 25 mL) at room temperature over 14 days. The resulting solution was filtered, leaving a white precipitate (KCl) and a colorless filtrate. Colorless crystals suitable for X-ray analysis precipitated from the solution after three weeks. Yield: 63%. IR (KBr, ν_{CN}, cm^{-1}) 2115(s).

Samples for elemental analysis were obtained by washing the crystals with dry hexane in a drybox and drying crystals under vacuum for 30 min. Four and a half DMF molecules per empirical unit were lost after washing and drying as determined by the elemental analysis. Anal. Calcd for $C_{73.5}H_{129.5}N_{36.5}O_{18.5}Cu_{12}La_2$: C = 30.85; H = 4.57; N = 17.87. Found: C = 30.71, H = 4.70, N = 17.56.

$\{$**[Eu(DMF)$_8$][Cu$_6$(CN)$_9$]·2DMF**$\}_\infty$**, 2.** The procedure was the same as that for **1**. $EuCl_3$ (317 mg, 1.23 mmol), CuCN (659 mg, 7.36 mmol), and KCN (240 mg, 3.69 mmol) in a 1:6:3 ratio were stirred in DMF (ca. 25 mL) at room temperature over 14 days. Yield: 56%. Anal. Calcd for $C_{39}H_{70}N_{19}O_{10}Cu_6Eu$: C = 31.26; H = 4.71; N = 17.76. Found: C = 30.97, H = 4.58, N = 17.23.

$\{$**[Er(DMF)$_8$][Cu$_6$(CN)$_9$]·2DMF**$\}_\infty$**, 4.** The procedure was the same as that for **1**. $ErCl_3$ (200 mg, 0.731 mmol), CuCl (217 mg, 2.19 mmol), and KCN (286 mg, 4.39 mmol) in a 1:3:6 ratio were stirred in DMF (ca. 25 mL) at room temperature over 14 days. The solution changed from yellow-greenish to colorless and eventually to pink. Light pink crystals formed after crystallization. Yield: 68%. Anal. Calcd for $C_{17}H_{28}N_9O_4Cu_2Er$: C = 30.95; H = 4.66; N = 17.58. Found: C = 30.60, H = 4.73, N = 17.43.

$\{$**La$_2$(DMF)$_8$Cu$_4$(CN)$_{10}$**$\}_\infty$**, 5.** $LaCl_3$ (200 mg, 0.815 mmol) and $KCu(CN)_2$ (378 mg, 2.44 mmol) in a 1:3 ratio were stirred in DMF (ca. 25 mL) at room temperature over 7 days. The resulting solution was filtered leaving a white precipitate (KCl) and a colorless filtrate. The DMF was pumped away to concentrate the solution, and colorless crystals were obtained the next day. Yield: nearly quantitative. IR (KBr, ν_{CN}, cm^{-1}): 2118(s). Anal. Calcd for $C_{17}H_{28}N_9O_4Cu_2La$: C = 29.66; H = 4.10; N = 18.31. Found: C = 28.96, H = 3.89, N = 17.33.

$\{$**Er$_2$(DMF)$_8$Cu$_4$(CN)$_{10}$**$\}_\infty$**, 7.** The procedure was the same as that for **5**. $ErCl_3$ (200 mg, 0.731 mmol) and $KCu(CN)_2$ (339 mg, 2.19 mmol) of in a 1:3 ratio were stirred in DMF (ca. 25 mL) at room temperature over 7 days. The resulting solution was filtered leaving a white precipitate (KCl) and a colorless filtrate. The DMF was pumped away to concentrate the solution, and colorless crystals were obtained the next day. Yield: nearly quantitative. IR (KBr, ν_{CN}, cm^{-1}): 2116(s,b). Anal. Calcd for $C_{17}H_{28}N_9O_4Cu_2Er$: C = 28.49; H = 3.94; N = 17.59. Found: C = 27.51, H = 4.22, N = 16.87.

$\{$**K(DMF)$_2$Cu(CN)$_2$**$\}_\infty$**, 8.** In a drybox, a 727 mg (11.2 mmol) quantity of KCN, 1000 mg (11.2 mmol) of CuCN, and 30 mL of DMF were charged into a flask. After stirring for 1 week, the solvent was removed on a vacuum line. A white crystalline powder (yield: nearly quantitative) was obtained. A crystal was picked from the recrystalization of $KCu(CN)_2$ in DMF for XRD.

Acknowledgment. This work was supported by the National Science Foundation through Grants CHE 99-01115 and CHE 02-13491.

Supporting Information Available: Supplementary molecular structures and solid state IR spectra. X-ray crystallographic files in CIF format of compounds **1**, **2**, **4**, **5**, **7**, and **8**. This material is available free of charge via the Internet at http://pubs.acs.org.

IC040113+

(17) Otwinowski, Z.; Minor, W. *Methods in Enzymology*; Carter, C. W., Jr., Sweet, R. M., Eds.; Academy Press: New York, 1997; Vol. 276-(A), p 307.

(18) (a) Blessing, R. H. *Acta Crystallogr., Sect. A* **1995**, *51*, 33−38. (b) Blessing, R. H. *J. Appl. Crystallogr.* **1997**, *30*, 421−426.

(19) Mackay, S.; Gilmore, C. J.; Edwards, C.; Tremayne, M.; Stuart, N.; Shankland, K. *MaXus: a computer program for the solution and refinement of crystal structures from diffraction data*; University of Glasgow: Scotland; Nonius BV: Delft; The Netherlands and MacScience Co. Ltd.: Yokohama, Japan, 1998.

(20) Sheldrick, G. M. *SHELXTL-97*: *A Structure Solution and Refinement Program*; University of Göttingen: Göttingen, Germany, 1998.